MR imaging of middle cerebral artery stenosis and occlusion: value of MR angiography.

N Fujita, N Hirabuki, K Fujii, T Hashimoto, T Miura, T Sato and T Kozuka

AJNR Am J Neuroradiol 1994, 15 (2) 335-341
http://www.ajnr.org/content/15/2/335

MR Imaging of Middle Cerebral Artery Stenosis and Occlusion: Value of MR Angiography

Norihiko Fujita, Norio Hirabuki, Keiko Fujii, Tsutomu Hashimoto, Takashi Miura, Tadayuki Sato, and Takahiro Kozuka

PURPOSE: To investigate the effectiveness of MR angiography in conjunction with spin-echo imaging for evaluating vascular patency in patients with middle cerebral artery (MCA) stenosis or occlusion. **METHODS:** Seven patients with MCA stenosis or occlusion, verified with contrast angiography in five and correlated with transcranial Doppler sonography in two, were examined using two-dimensional and/or three-dimensional time-of-flight MR angiographic techniques as well as conventional spin-echo imaging. **RESULTS:** Of the seven patients, six demonstrated basal ganglionic and/or cortical infarct in the MCA territory. Except one case with minimal stenosis immediately distal to the MCA origin, all six cases with either severe stenosis or occlusion of the main trunk of the MCA showed the absence of normal flow voids using spin-echo imaging in the sylvian fissure on the affected side. However, it was not possible to discriminate between stenosis and occlusion. Although different mechanisms (ie, flow-induced spin dephasing for the 2-D technique and progressive spin saturation for the 3-D technique) were predominantly responsible for the loss of signal through the area of stenosis, both the 2-D and 3-D MR angiograms clearly depicted the compromised flow of the MCA: a focal discontinuity with decreased vessel caliber corresponded to stenosis, and nonvisualization of distal MCA branches represented occlusion. **CONCLUSION:** Either 2-D or 3-D time-of-flight MR angiography is a useful adjunct to conventional parenchymal spin-echo imaging for evaluating vascular patency in patients with MCA stenosis or occlusion, although it is important to recognize that each technique has a different basis for the loss of signal through the area of stenosis.

Index terms: Arteries, cerebral, middle (MCA); Arteries, stenosis and occlusion; Arteries, magnetic resonance angiography (MRA); Arteries, magnetic resonance

AJNR Am J Neuroradiol 15:335–341, Feb 1994

Within the frame of evaluating the effectiveness of a variety of magnetic resonance (MR) angiographic techniques, studies have described primary stenosis or occlusion of intracranial arteries (1–4); however, most were limited to a few anecdotal cases. We examined seven cases with middle cerebral artery (MCA) stenosis or occlusion, verified with contrast angiography in five cases and correlated with transcranial Doppler sonography in two cases, using two-dimensional and/or three-dimensional time-of-flight MR angiographic techniques as well as conventional spin-echo imaging. The purpose of this study was to investigate the effectiveness of time-of-flight MR angiography in combination with spin-echo imaging for evaluating patients with primary stenosis or occlusion of the MCA.

Patients and Methods

All seven patients in this study had experienced hemiplegia that led to neurologic evaluation and subsequent cerebral angiography or Doppler sonography (Table 1). The group included three children and four adults. Of five patients who had cerebral angiography, three presented with stenosis of the horizontal segment of the MCA and two with occlusion immediately distal to the MCA origin. Two patients who did not have cerebral angiography were examined with transcranial Doppler sonography. One of the two patients showed no flow pattern of the left MCA, and the remaining one no flow pattern of the bilateral

Received October 12, 1992; accepted pending revision January 5, 1993; revision received March 11.

From the Department of Radiology (N.F., T.S.), Suita Municipal Hospital, Osaka, Japan; and the Department of Radiology (N.F., N.H., K.F. T.H., T.M., T.K.), Osaka University Medical School, Osaka, Japan.

Address reprint requests to Norihiko Fujita, MD, Department of Radiology, Suita Municipal Hospital, 2–13–20, Katayama-Cho, Suita-City, Osaka 564, Japan.

AJNR 15:335–341, Feb 1994 0195-6108/94/1502–0335

TABLE 1: Summary of patients with MCA stenosis or occlusion

Case	Age/Sex	Angiographic Findings	Findings on Spin-Echo Images		MR Angiographic Findings of the affected MCA
			Location of Infarct	Normal Flow Void in the Sylvian Fissure	
1	2/M	Minimal narrowing of right M1	Right basal ganglia	Present on both sides	Discontinuity (2-D, 3-D)
2	36/M	Severe narrowing of left M1	None seen	Absent on the left	Discontinuity (2-D)
3	64/F	Left MCA occlusion	Left basal ganglia	Absent on the left	Nonvisualization (2-D, 3-D)
4	60/F	Not done[a]	Left basal ganglia	Absent on both sides	Nonvisualization on both sides (2-D, 3-D)
5	2/M	Severe narrowing of left M1 and internal carotid artery	Left basal ganglia	Absent on the left	Discontinuity (2-D) Nonvisualization (3-D)
6	11/M	Not done[a]	Left basal ganglia + cortex	Absent on the left	Discontinuity (2-D, 3-D)
7	58/M	Right MCA occlusion	Right basal ganglia + cortex	Absent on the right	Nonvisualization (2-D, 3-D)

M1 indicates horizontal segment of MCA.

[a] In cases 4 and 6, contrast angiography was not done because of history of preleukemic state and previous surgery for congenital heart disease, respectively. Both cases underwent transcranial Doppler sonography, which revealed no flow pattern of the bilateral MCAs for case 4 and the left MCA for case 6.

MCAs. Of the seven patients, three (cases 2, 3, and 7) were referred for MR imaging of the brain based on the angiographic findings. For the remaining four patients who were observed on MR to have suspected MCA stenosis/occlusion, they had angiography or transcranial Doppler sonography to confirm MR findings.

All patients were studied on a 1.5-T MR unit (Magnetom, Siemens, Erlangen, Germany) using 2-D and/or 3-D time-of-flight MR angiography and spin-echo imaging. Imaging parameters for spin-echo pulse sequences were 630/15/2 (repetition time/echo time/excitations) for T1-weighted images and 2500/15–90/1 for proton-density- and T2-weighted images, respectively. The section thickness was 5–6 mm with an intersection gap varying from 10% to 15%. The acquisition matrix was 192 × 256 and the field of view 21 cm. Axial proton-density- and T2-weighted images and axial and/or coronal T1-weighted images were obtained. The MR scans were done 24 to 69 days (mean 38.5 days) during the chronic stage after clinical presentation of stroke. During either the acute or subacute stage, computed tomographic scans and/or transcranial Doppler sonography were done. Five of the seven patients had contrast cerebral angiography in our institution within 6 days of the MR scans.

MR angiograms were obtained by using 2-D and/or 3-D time-of-flight techniques immediately after the spin-echo imaging. In all patients were obtained 2-D time-of-flight MR angiograms consisting of the sequential section acquisition with a gradient-echo pulse sequence and postprocessing from the stack of 2-D sections by a maximum intensity projection algorithm. The pulse sequence used for 2-D time-of-flight MR angiography was a spoiled gradient-echo sequence that was first-order gradient moment nulled in the section and read directions. The imaging parameters were 80/7/1, 90° flip angle, 192 × 256 matrix, 21-cm field of view, and 3-mm section thickness. In all patients, consecutive axial and/or coronal sections were obtained. Depending on the anatomic extent of interest, the number of sections was varied in the range of 9 to 17. MR angiograms projected in the section direction were obtained for either axial or coronal acquisition using a maximum intensity projection algorithm.

In six of the seven patients, 3-D time-of-flight MR angiograms were also obtained. We used a fast low-angle shot or fast imaging with steady precession pulse sequence with first-order flow compensation in the read and section directions. The imaging parameters were 45–60/7/1, 25° to 35° flip angle, 192 × 256 matrix, and 21-cm field of view. The excitation slab was a 32- to 45-mm axial slab with 32 partitions, which was usually centered at the level of the circle of Willis. MR angiograms projected in the axial direction were created from each set of 3-D data by using a maximum intensity projection algorithm.

The spin-echo images and MR angiograms were assessed with particular reference to the evaluation of vascular patency of the MCAs. The proton-density- and T2-weighted axial spin-echo images were primarily analyzed for presence of normal flow void of the MCAs. In particular, the segments perpendicular to the axial plane of section (ie, the branches in the sylvian fissure rather than the horizontal segment) were evaluated to avoid the partial volume effects. For evaluating MR angiograms, the original 2-D or 3-D sections were not used, but the reformatted images projected in the axial plane were primarily used. The MCAs seen on either 2-D or 3-D MR angiogram were evaluated with respect to the size of the vessel caliber, the

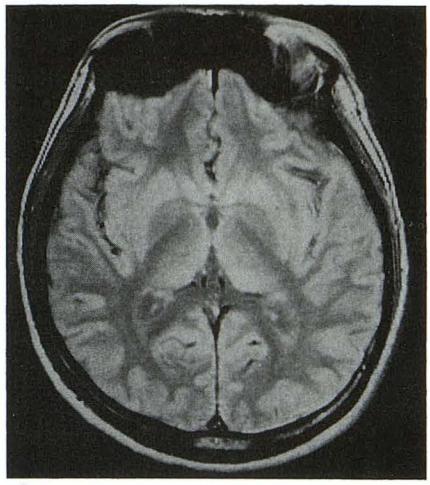

A

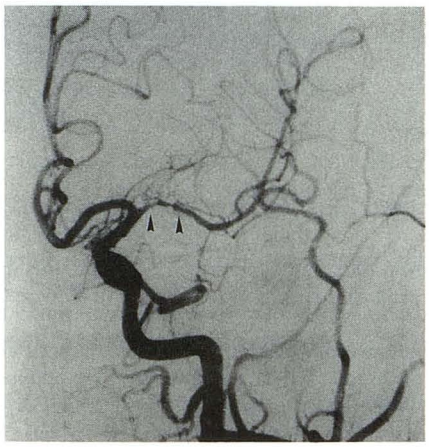

B

C

Fig. 1. Case 2: 36-year-old man with transient right-sided weakness and dysphasia. No parenchymal abnormalities were recognized on spin-echo images at the time of MR examination 24 days after his symptomatology.

A, Proton-density–weighted spin-echo image (2500/15) at the level of the basal ganglia shows the absence of normal flow voids in the left sylvian fissure, indicating the presence of compromised flow of the ipsilateral MCA.

B, Left carotid angiogram shows severe narrowing of the proximal portion of the left MCA (*arrowheads*).

C, Two-dimensional MR angiogram (80/7, 90° flip angle) shows an apparent discontinuity (*arrows*) of the left proximal MCA with distal portion of linear high intensity.

presence or absence of focal discontinuities, and the extent of visualization.

Results

The findings are presented in Table 1. Of the seven patients, six demonstrated basal ganglionic and/or cortical infarcts in the MCA territory. In the remaining one patient (Fig 1, case 2), who had a transient hemiplegia and no neurologic deficit at the time of the MR examination 24 days after his symptomatology, no parenchymal abnormalities were found. In four cases with occlusion and two with severe stenosis of the MCA, the absence or obscuration of normal flow voids in the sylvian fissure and/or the main trunk of the MCA on the affected side was recognized on the spin-echo images. In the remaining one case (Fig 2, case 1) with minimal narrowing of the MCA, of which diagnosis was confirmed with contrast angiography, no vessel abnormalities were found on the spin-echo images despite the presence of basal ganglionic infarct.

Although the 2-D time-of-flight MR angiograms tended to exaggerate the extent of stenosis because of the elongated voxel size in the section direction, overall, both the 2-D and 3-D MR angiograms correctly demonstrated the compromised flow of the MCA; an apparent discontinuity with decreased vessel caliber corresponded to stenosis, and nonvisualization of distal MCA branches represented occlusion (eg, Fig 3, case 7). In one case with severe stenosis (Fig 4, case 5), there was a discrepancy between the 2-D and 3-D MR angiographic findings; the 2-D angiogram showed a decreased caliber of the horizontal segment of the left MCA with a focal discontinuity, compatible with stenosis, but the 3-D angiogram demonstrated nonvisualization of the distal portion of the horizontal segment, leading to an incorrect diagnosis of occlusion.

Discussion

MR imaging offers a major advance in evaluating cerebral ischemia not only because of its superior sensitivity for the detection of infarcted areas but also because of its ability to depict vascular lumina by exploiting flow phenomena inherent to the MR methodology.

The characteristic flow void, seen as the absence of signal on spin-echo images, indicates vascular patency and rapid flow; an absence of this finding strongly suggests either complete occlusion or slow flow. The evaluation of flow void on spin-echo images, which costs no addi-

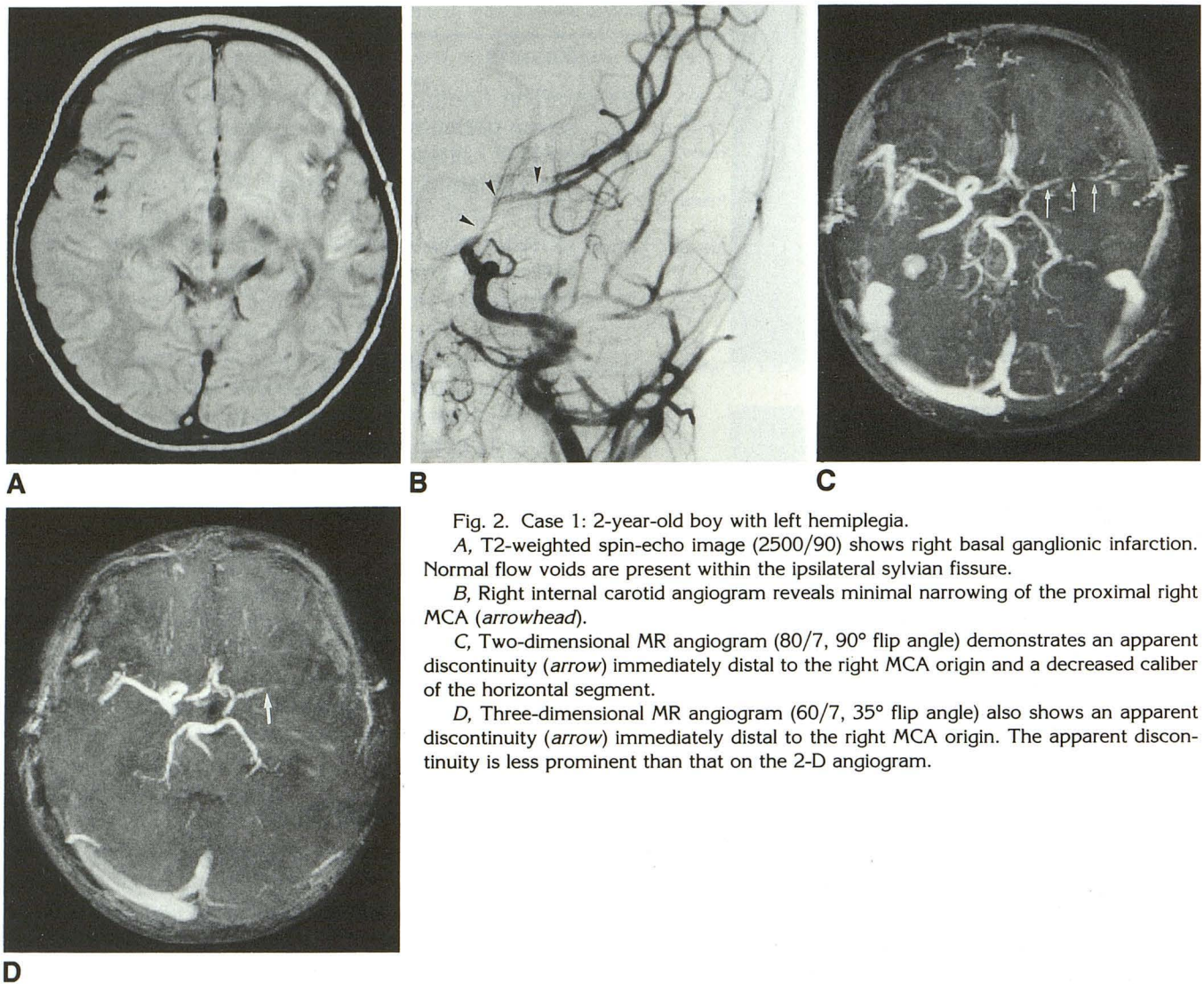

Fig. 2. Case 1: 2-year-old boy with left hemiplegia.

A, T2-weighted spin-echo image (2500/90) shows right basal ganglionic infarction. Normal flow voids are present within the ipsilateral sylvian fissure.

B, Right internal carotid angiogram reveals minimal narrowing of the proximal right MCA (*arrowhead*).

C, Two-dimensional MR angiogram (80/7, 90° flip angle) demonstrates an apparent discontinuity (*arrow*) immediately distal to the right MCA origin and a decreased caliber of the horizontal segment.

D, Three-dimensional MR angiogram (60/7, 35° flip angle) also shows an apparent discontinuity (*arrow*) immediately distal to the right MCA origin. The apparent discontinuity is less prominent than that on the 2-D angiogram.

tional imaging time for depicting vascular lumina, seems simple and unambiguous. However, previous studies using spin-echo imaging in assessing the patency of the internal carotid artery (5–8) have suggested that the intraluminal signal changes of compromised flow of the internal carotid artery are considerably inconsistent. For instance, it is highly likely that complete isointense signal of the internal carotid artery corresponds to complete occlusion, but the combination of time-of-flight effects and flow-induced phase-shift effects may produce isointensity in a slow-flow state (7) and even in a normal flow state in a specific condition that depends on vessel and imaging axis orientation (9).

Considering the small size of the vessel and the expected variabilities of the intraluminal signal intensities caused by the various flow phenomena, we determined only the presence or absence of normal flow voids in the sylvian fissure irrespective of their intraluminal signal intensities. In our series, all six cases with either severe stenosis or occlusion of the MCA showed absence of normal flow voids in the sylvian fissure on the affected side. Spin-echo imaging could demonstrate the presence of an abnormality by depicting absence of flow voids within MCA branches, but this finding was nonspecific and could not distinguish between stenosis and occlusion. Furthermore, in one case (case 1) who presented with minimal narrowing of the main trunk of the MCA, no vessel abnormalities were found on the spin-echo images (Fig 2A). This may be explained by the assumption that such a hemodynamically insignificant stenosis provides an almost normal distal flow, leading to normal flow voids in the

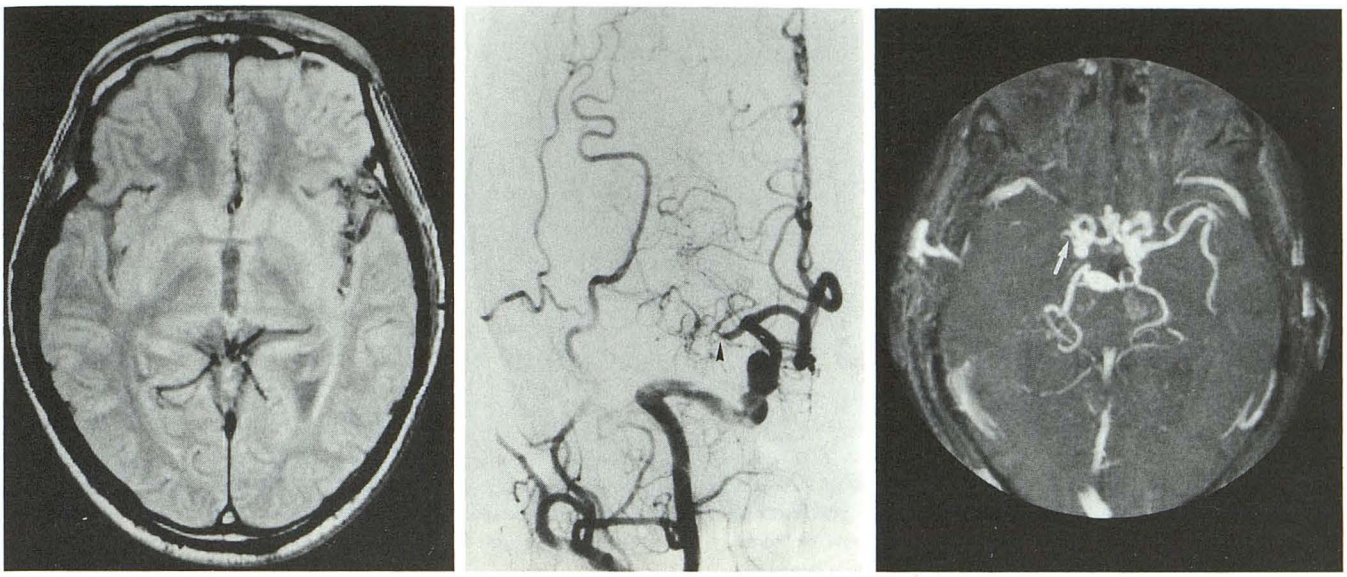

Fig. 3. Case 7: 58-year-old man with left hemiplegia and dysphasia and basal ganglionic and cortical infarcts in the right MCA territory documented on spin-echo images.

A, Proton-density–weighted spin-echo image (2500/15) at the level of the basal ganglia shows disappearance of normal flow voids in the right sylvian fissure.

B, Right common carotid angiogram shows occlusion of the right MCA (*arrowhead*).

C, Three-dimensional MR angiogram (50/7, 25° flip angle) demonstrates nonvisualization of the right MCA (*arrow*).

sylvian fissure. It is obvious that spin-echo imaging is useful in demonstrating the presence or absence of associated cerebral infarction and as a screening technique to demonstrate the presence of normal flow voids. When normal flow voids are absent or in cases of clinically suspected vascular stenosis or occlusion, it is necessary to pursue the patient study further with the use of MR angiography.

Compared with the evaluation of vascular patency with spin-echo imaging, the depiction of vascular stenosis and occlusion with time-of-flight MR angiographic techniques is straightforward. In our series, both 2-D and 3-D MR angiographic findings demonstrated the compromised flow of the MCA; apparent discontinuity with decreased vessel caliber and nonvisualization of distal MCA branches corresponded to stenosis and occlusion, respectively, in most cases.

However, there were minor differences recognized in the depiction of the compromised flow of the MCA between the 2-D and 3-D MR angiograms. These differences are thought to reflect advantages and disadvantages inherent to each technique. First, in one case (case 1) with minimal stenosis of the main trunk of the MCA, the extent of the apparent discontinuity through the area of stenosis was exaggerated on the 2-D angiogram compared with the 3-D angiogram, as shown in Figures 2C and 2D. This apparent discontinuity, seen in all three cases with either minimal or severe stenosis, results from flow-induced intravoxel dephasing through the area of stenosis where the rapid acceleration of spins occurs. Signal loss caused by flow-induced spin dephasing can be reduced with the use of smaller voxel sizes as well as shorter echo times and gradient moment nulling. We used the same echo time of 7 with first-order gradient moment nulling for both 2-D and 3-D time-of-flight techniques, but the section thickness of 3 mm for the 2-D technique was more than twice as thick compared with the 3-D technique. This would increase the vulnerability to flow-induced dephasing for the 2-D technique, resulting in the exaggeration of the apparent discontinuity through the area of stenosis.

Second, in one case (case 5) with severe stenosis of the MCA, the 2-D MR angiogram (Fig 4C) showed a decreased caliber size of the horizontal segment of the left MCA with a focal discontinuity, compatible with stenosis, whereas the 3-D MR angiogram (Fig 4D) showed nonvisualization distal to the midportion of the horizontal segment, leading to an incorrect diagnosis of occlusion. This discrepancy is thought to reflect the difference in the effects of progressive spin saturation between the 2-D and 3-D time-of-flight

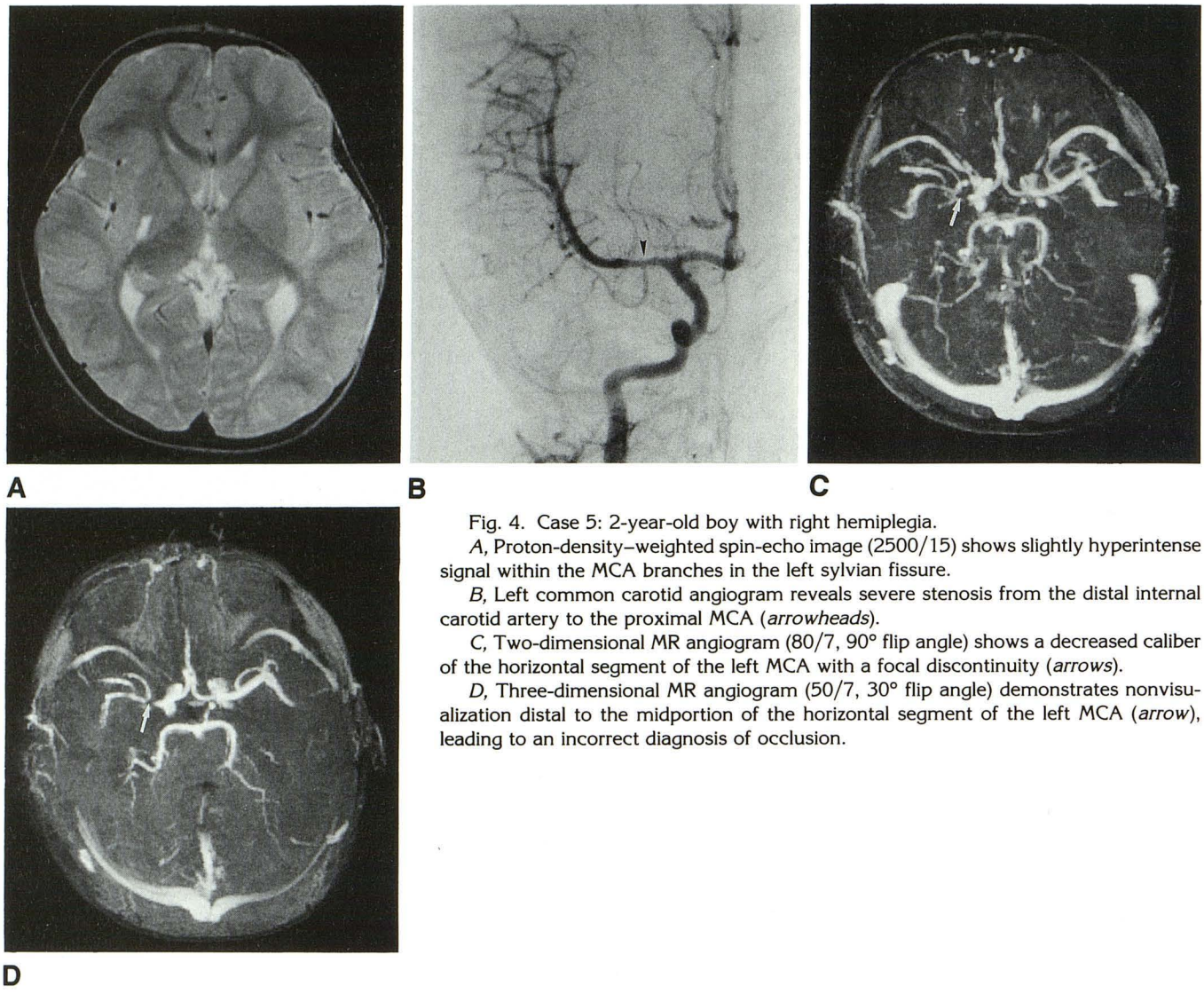

Fig. 4. Case 5: 2-year-old boy with right hemiplegia.

A, Proton-density–weighted spin-echo image (2500/15) shows slightly hyperintense signal within the MCA branches in the left sylvian fissure.

B, Left common carotid angiogram reveals severe stenosis from the distal internal carotid artery to the proximal MCA (*arrowheads*).

C, Two-dimensional MR angiogram (80/7, 90° flip angle) shows a decreased caliber of the horizontal segment of the left MCA with a focal discontinuity (*arrows*).

D, Three-dimensional MR angiogram (50/7, 30° flip angle) demonstrates nonvisualization distal to the midportion of the horizontal segment of the left MCA (*arrow*), leading to an incorrect diagnosis of occlusion.

techniques. The inferior sensitivity of the 3-D technique to the depiction of flow distal to stenosis is attributable to the inability of pathologically slowed arterial flow to span the entire volume before becoming sufficiently saturated to prevent visualization. Because of its slow flow sensitivity, the 2-D technique is more suitable for the depiction of flow distal to stenosis similar to its ability to image slowly flowing veins (10, 11).

The loss of signal through the region of stenosis in time-of-flight MR angiography is caused by the factors: flow-induced spin dephasing and progressive spin saturation. In general, the 2-D time-of-flight technique with inferior spatial resolution in the section direction is more vulnerable to the spin-dephasing effects than the single-volume 3-D time-of-flight technique; the former is less affected by the progressive spin saturation. To combine the strengths of both the 2-D and 3-D techniques, the multiple overlapping thin slab acquisition technique has been developed (4, 11–13). However, this approach has its own disadvantage of the variation in signal intensity at slab boundaries. Artifacts from signal variation or patient motion may result in discontinuities at slab boundaries, which may be misinterpreted as stenosis.

In conclusion, spin-echo imaging can show the absence of normal flow voids in the sylvian fissure in hemodynamically significant stenosis or occlusion of the MCA. This should prompt further study of MR angiography. MR angiography is a useful adjunct that in many cases can depict the site of stenosis or occlusion and distinguish between these two entities. However, for proper interpretation of the MR angiographic studies, it is important to recognize that 2-D and 3-D time-of-flight MR angiographic techniques may have

a different basis for signal loss through the area of stenosis.

References

1. Masaryk TJ, Modic MT, Ross JS, et al. Intracranial circulation: preliminary clinical results with three-dimensional (volume) MR angiography. *Radiology* 1989;171:793–799
2. Wagle WA, Dumoulin CL, Souza SP, Cline HE. 3DFT MR angiography of carotid and basilar Arteries. *AJNR Am J Neuroradiol* 1989;10:911–919
3. Masaryk TJ, Laub GA, Modic MT, Ross JS, Haacke EM. Carotid-CNS MR flow imaging. *Magn Reson Med* 1990;14:308–314
4. Blatter DD, Parker DL, Ahn SS, et al. Cerebral MR angiography with multiple overlapping thin slab acquisition: part II. Early clinical experience. *Radiology* 1992;183:379–389
5. Katz BH, Quencer RM, Kaplan JO, et al. MR imaging of intracranial carotid occlusion. *AJNR Am J Neuroradiol* 1989;10:345–350
6. Heinz ER, Yeates AE, Djang WT. Significant extracranial carotid stenosis: detection on routine cerebral MR images. *Radiology* 1989;170:843–848
7. Brant-Zawadzki M. Routine MR imaging of the internal carotid artery siphon: angiographic correlation with cervical carotid lesions. *AJNR Am J Neuroradiol* 1990;11:467–471
8. Lane JI, Flanders AE, Doan HT, Bell RD. Assessment of carotid artery patency on routine spin-echo MR imaging of the brain. *AJNR Am J Neuroradiol* 1991;12:819–826
9. Fujita N, Harada K, Hirabuki N, et al. Asymmetric appearance of intracranial vessels on routine spin-echo MR images: a pulse sequence-dependent phenomenon. *AJNR Am J Neuroradiol* 1992;13:1153–1159
10. Mattle HP, Wentz KU, Edelman RR, et al. Cerebral venography with MR. *Radiology* 1991;178:453–458
11. Lewin JS, Laub G. Intracranial MR angiography: a direct comparison of three time-of-flight techniques. *AJNR Am J Neuroradiol* 1991;12:1133–1139
12. Parker DL, Yuan C, Blatter DD. MR angiography by multiple thin slab 3D acquisition. *Magn Reson Med* 1991;17:434–451
13. Blatter DD, Parker DL, Robison RO. Cerebral MR angiography with multiple overlapping thin slab acquisition: part I. Quantitative analysis of vessel visibility. *Radiology* 1991;179:805–811